

# Fog spatial distributions over the Central Namib Desert - an isotope approach

Kudzai Farai Kaseke<sup>1</sup>, Chao Tian<sup>1</sup>, Lixin Wang<sup>1\*</sup>, Mary Seely<sup>2,3</sup>, Roland Vogt<sup>4</sup>,  
Theo Wassenaar<sup>3</sup>, Roland Mushi<sup>3</sup>

<sup>1</sup> *Department of Earth Sciences, Indiana University-Purdue University Indianapolis, Indianapolis, IN 46202, USA*

<sup>2</sup> *Desert Research Foundation of Namibia, 7 Rossini Street, Windhoek, Namibia*

<sup>3</sup> *Gobabeb Research and Training Centre, Walvis Bay, Namibia*

<sup>4</sup> *Research Group Meteorology, Climatology, and Remote Sensing, University of Basel, Basel, Switzerland*

## Abstract

Fog is a characteristic feature of the Namib Desert and is essential to life in this fog dependent system. It is often acknowledged that advective fog is the dominant fog type over the Namib Desert fog-zone but recent evidence suggests that other fog types occur in this area. Knowledge of the existence and spatial distribution of different fog types will enhance the mechanistic understanding of fog formation and potential changes in this region, but such knowledge is limited in literature. In this study, we investigated fog spatial variations within the Namib Desert fog-zone by applying stable isotope ( $\delta^{18}\text{O}$  and  $\delta^2\text{H}$ ) techniques to differentiate various fog types and identify their source waters. Isotope based results showed that at least three types of fog (advective, radiation and mixed) occurred in this region and what appears as a single fog event may include all three types. Results suggest that radiation fog was the dominant fog type during our study period. The results also suggest that advective fog (with Atlantic Ocean origins) either dissipated 30-50 km inland and the residual humidity combined with locally derived moisture to form mixed fog or advective fog incorporated local moisture along its trajectory inland resulting in mixed fog. Fog in the Namib Desert was consistently depleted in  $^{18}\text{O}$  and  $^2\text{H}$  compared to rainfall and this was attributed to sub-cloud evaporation of the rainfall as well as different sources of fog and rainfall. Sub-cloud evaporation led to enrichment of  $^{18}\text{O}$  and  $^2\text{H}$  in rainfall beyond that of the first stage condensate, fog. Advective fog is often considered the architect of the fog-zone in the Namib Desert, but our results demonstrated multiple dominant fog types during the study period, suggesting knowledge of both fog frequency and fog type is needed to better predict climate change impacts on the fog-zone.

**Keywords:** Advective; Climate change; Ecohydrology, Isotopes; Mixed; Radiation;  $\delta^{18}\text{O}$ ;  $\delta^2\text{H}$

## INTRODUCTION

Non-rainfall waters (e.g., fog and dew) are the least studied hydrological components in most ecosystems. However, these non-rainfall water components play an important role in ecosystem dynamics and are particularly important for water-limited ecosystems (Wang et al., 2016). In arid ecosystems, non-rainfall waters can exceed rainfall and can be the sole source of water for plants (Agam and Berliner, 2006), thus the ecophysiology of these organisms is geared towards obtaining non-rainfall waters (Henschel and Seely, 2008).

According to Byers (1959), it is challenging to provide an exact definition of fog because fog formation occurs under a variety of conditions and is dependent on the observer's perspective and research interests (George, 1951; Tardif and Rasmussen, 2007). However, for practical purposes, fog is defined as the suspended water droplets or ice crystals that are near the surface and lead to horizontal visibility below 1 km (WMO, 1992). Fog formation is influenced by thermodynamic or radiative cooling, aerosol concentration, microphysical processes and surface conditions (Gultepe et al., 2007a), thus classification is often based on different combinations of these factors. George (1951) restricted fog classification to six categories: advection, radiation (restricted heating or air drainage), advection-radiation, pre-warmfrontal and mixed radiation. However, given the location of the Central Namib Desert (the region of interest in this study), the first three categories are of interest, thus we present general definitions of these categories.

Advection fog is formed in one area and transported to the site of interest (Degefie et al., 2015).

Radiation fog is formed from radiative cooling of stagnant air close to the surface (Gultepe et al., 2007b). Advection-radiation fog occurs in coastal areas and is formed from the advection of moist air inland during daylight hours followed by radiative cooling (Ryznar, 1977).

Fog has been recognized as an important component of hydrologic and nutrient cycling in forest ecosystems of coastal areas (Weathers and Likens, 1996; Dawson, 1998; Wang et al., 2016). It is often assumed that fog in these coastal regions is advected from the ocean and the majority of authors agree that advective sea fog dominates the south-west coast of Africa (Seely, 1979; Olivier, 2004; Jacobson et al., 2015). The most visible impacts of this advective fog on ecophysiology in the Namib Desert are thought to extend about 60 km inland, a region known as the fog-zone (Seely, 1979; Lancaster, 1984; Olivier, 1995). However, recent studies show that other fog types may be a regular occurrence in the Namib fog-zone, especially along ephemeral rivers and other low laying areas (Eckardt et al., 2013; Kaseke et al., 2017). Therefore we could be under-estimating the significance of other fog types, which hinders the understanding of the potential impact of global climate change on these fog dominated environments.

Despite the ecohydrological significance of fog to many arid and semi-arid ecosystems, coastal regions and tropical montane forests (Schemenauer and Cereceda, 1991; Dawson, 1998; Ebner et al., 2011; Nørgaard et al., 2012), we still do not fully understand the spatial variation and/or

origin of fog in these environments. Cereceda et al. (2002) suggests advective fog in the Atacama Desert dissipates and persists as an area of high humidity, which can be transported further inland. If the high humidity is radiatively cooled, it can result in localized condensation and forms radiation fog (some would call it advection-radiation fog (George, 1951; Ryznar, 1977)). Alternatively, inland fog could be generated from condensation of localized evaporation from the salt flats of the Atacama Desert and classified as radiation fog (Cereceda et al., 2002). The inland fog could also be generated from possible mixing of different air masses to form mixed fog (Degeffie et al., 2015). Therefore, in addition to the traditional fog classification techniques, there is a critical need for an objective method that will enable reliable fog differentiation over a large geographic area.

Stable isotopes are one of the best tools available to trace fog water movement because isotope fractionation imparts unique signatures that can be used as environmental tracers (Ingraham and Matthews, 1988). Over the years, stable isotopes have been successfully applied to different fog studies and have shown that in some environments fog contributes to groundwater recharge (Ingraham and Matthews, 1988, 1990; Scholl et al., 2002) and vegetation water use (Dawson, 1998; Limm et al., 2009; Simonin et al., 2009). Although the spatial variation of fog has been investigated at some sites (Tardif and Rasmussen, 2007; Bari et al., 2016), the classification methods are often based on subjective algorithms. As George (1951) points out that there will

always be exceptions to classification based on meteorology or aviation forecasting. Here we utilize a classification system based on the isotope approach composed of three fog classes: advective (externally sourced), radiation (locally generated), mixed fog (advection + radiation). The objectives of this study were to identify the fog classes of each fog event at multiple sites, identify source waters of different fog types during each fog event and understand the spatial distribution of these fog types within the Namib Desert.

## **METHODS**

### ***Site description***

This study was conducted in the central Namib Desert located on the south-western edge of the summer rainfall zone (Schulze, 1969) (Fig. 1). The central Namib Desert receives less than 25 mm annual rainfall (Eckardt et al., 2013), while the western half receives less than 12 mm (Henschel and Seely, 2008), resulting in an east-west decreasing rainfall gradient (Lancaster, 1984; Hachfeld et al., 2000). Fog occurs throughout the year but peak seasons differ between the coast and the interior. The peak fog season for the coast is winter while that for the interior is summer. However, the greatest fog intensity for all sites is between June and July (Lancaster, 1984). There is a west-east gradient with decreasing fog frequency (Lancaster, 1984). Rainfall and groundwater availability are often the primary determinants of species distribution in the Namib Desert (Schachtschneider and February, 2010), with large trees confined to the eastern

edge of the desert and along ephemeral water courses (Burke, 2006) where they access the shallow alluvial aquifers (Lange, 2005). The sampling sites were located between the Swakop and Kuiseb ephemeral rivers (Fig. 1).

**[Figure 1 here]**

Fog samples were collected from a total of 13 stations. Eight stations were part of the Southern African Science Service Centre for Climate Change and Adaptive Land Management (SASSCAL) or FogNet (FN) project, while the remaining five were temporary stations (Fig. 1 and Table S1). The FN stations were equipped with automated meteorological instrumentation along with a passive cylindrical fog collector facilitating fog collection and correlation with local meteorological conditions (Fig. 1). Data was recorded at hourly intervals from the FN stations and consisted of wind speed, air temperature, soil temperature (10 cm depth), rainfall, relative humidity (RH) and leaf wetness. Because atmospheric pressure was only recorded at Coastal MET FN and Vogelfederberg FN stations, specific humidity was only computed for these two stations. Each temporary station (station 1 to 5) consisted of a passive flat fog collector (1m<sup>2</sup>) after Schemenauer and Cereceda (1994) and was established primarily to increase spatial sampling coverage. The total area covered by all fog stations was about 1700 km<sup>2</sup> and a roundtrip visit was about 250 km (Fig. 1). Fieldwork was conducted from the 9<sup>th</sup> June – 22<sup>nd</sup> June 2016 and involved daily site visits to all stations to inspect and collect fog samples (Fig. 1). Fog events

were identified by the presence of sample in the fog collectors. At the FN stations this was in conjunction with wetness recorded on the leaf wetness sensor (0.1 m). The leaf wetness data enabled determination of the duration of the fog event and associated meteorological conditions. Fog samples were transferred into 15 ml Qorpak clear French square bottles with black phenolic polycone lined caps, labelled appropriately with the sample type, location and date and stored at the Gobabeb Research and Training Centre (Gobabeb), until they were shipped to Indiana University-Purdue University Indianapolis (IUPUI) Ecohydrology Lab for isotope analysis.

We used a Triple Water Vapor Analyzer (Los Gatos Research Inc., Mountain View, CA, USA), for isotopic analysis with a precision of 0.2‰  $\delta^{18}\text{O}$  and 0.8‰  $\delta^2\text{H}$  similar to those reported elsewhere (Wang et al., 2009). Data was reported in  $\delta$  notation relative to VSMOW-SLAP scale as

$$\delta = \frac{R_{\text{sample}}}{R_{\text{VSMOW}}} - 1 \quad , \quad (1)$$

where  $R_{\text{sample}}$  and  $R_{\text{VSMOW}}$  are the molar ratios of heavy to light isotopes ( $^2\text{H}/\text{H}$  or  $^{18}\text{O}/^{16}\text{O}$ ) of the sample and international standard - Vienna Standard Mean Ocean Water (VSMOW).

### ***Differentiation of fog sources based on isotopes***

Isotope fractionation imparts unique signatures on meteoric water that can be combined with deuterium excess, defined as  $d = \delta^2\text{H} - 8 \times \delta^{18}\text{O}$  (Dansgaard, 1964), to determine source origins and evaporative conditions (Merlivat and Jouzel, 1979). Because fog is a first-stage condensate

controlled by equilibrium fractionation processes, it should plot on a meteoric water line reflecting its origins (Gonfiantini and Longinelli, 1962; Majoube, 1971; Stewart, 1975; Jouzel, 1986). We thus assumed fog formed from oceanic vapour would plot on the global meteoric water line (GMWL), fog formed from local meteoric waters on the local meteoric water line (LMWL) and fog formed from a mixture of the two air masses would plot between the two meteoric water lines (Kaseke et al., 2017). Since transpiration and equilibrium fractionation do not alter  $d$  (Dansgaard, 1964; Gat, 2005), fog  $d$  derived from transpired vapor would be similar to LMWL  $d$ , while advective  $d$  would be similar to that of GMWL, +10‰. However, because evaporation increases  $d$  of vapor relative to evaporating water (Salati et al., 1979; Gat and Matsui, 1991), fog formed from evaporated vapor should have a larger  $d$  than the LMWL. Therefore if radiation fog plots on the LMWL we assume it did not undergo evaporative enrichment after formation. If its  $d$  is smaller or equal to the LMWL  $d$ , this suggests transpiration is the main vapor transport pathway and transpired vapor is used for fog formation. If its  $d$  is larger than the LMWL, this suggests a significant contribution of vapor from evaporation of local water sources. Admixture of different air masses will lead to significantly greater  $d$  compared to LMWL  $d$  (Gat and Matsui, 1991; Martinelli et al., 1996; Liu et al., 2007), thus we expect mixed fog  $d$  to have a larger  $d$  than LMWL. From Kaseke et al. (2017), despite being transported 60 km inland, advective fog plotted around the GMWL and had an isotopic composition similar to that sampled



from the coast. Therefore, we should be able to identify advective fog isotopically from all sampling sites as the furthest sites were located about 60 km inland (Fig. 1).

Because the stations were remote and receive similar amounts of rainfall, typically less than 20 mm annual rainfall (Henschel and Seely, 2008), defining a LMWL for each site would be challenging. Instead, we assumed similar meteorological conditions across the sites given their close proximity (Fig. 1). This assumption enabled the application of the LMWL defined for Gobabeb,  $\delta^2\text{H} = 7.01 \times \delta^{18}\text{O} - 0.6$  (Kaseke et al., 2017), to all sites. This LMWL was generated from precipitation, ephemeral water and groundwater samples obtained from Gobabeb (2014 - 2015) and excluded fog and dew. Because transpiration is non-fractionating, transpired vapor is isotopically similar to source waters (Wang et al., 2010; Wang et al., 2012), hence groundwater was included to the LMWL to account for possible vegetation groundwater uptake along the riverbeds (Fig.1).

### ***Trajectory analyses***

All FN stations received rainfall on the 6<sup>th</sup> and 7<sup>th</sup> June 2016, supporting the assumption of similar meteorological conditions across sites (Table 1). Hybrid Single Particle Lagrangian Trajectory Model (HYSPLIT) (Stein et al., 2015) was used to model the origin of these rain events for each of the FN stations. Based on the data from each FN station, we calculated dewpoint temperature (Berry et al., 1945) at the start of the rainfall event at each station. We used

this value to calculate an approximate cloud height, lifted condensation level (LCL), for the rain event at the station. The back-trajectory of the rain producing air-mass was then computed based on the LCL to identify origins (Soderberg et al., 2013). However, because there may be microclimatological differences among sites, we analysed air temperature, soil temperature and RH among sites and classified the sites into two groups: northern (Coastal MET, Kleinberg, Station 3, Station 4, Sophies Hoogte and Marble Koppie) and southern sites (Vogelfederberg, Station 8, Aussinanis, Gobabeb, Station 1, Station 2 and Station 5,) (Fig. 1). Statistical analysis was performed in PAST 3 (Paleontological Statistics, Natural History Museum, University of Oslo), with parametric methods for normally distributed data and non-parametric methods for non-normally distributed data.

## **RESULTS AND DISCUSSION**

### ***Classification of fog on the 10<sup>th</sup> June 2016***

Sufficient sample for isotopic analysis on the 10<sup>th</sup> June 2016 was obtained from eleven of the twelve sites (station 5 was not set up yet). Nine of these fog samples plotted on the LMWL, suggesting they were derived from local meteoric waters (Fig. 2). These samples were defined by the regression line  $\delta^2\text{H} = 6.17 \times \delta^{18}\text{O} - 1.2$  and we did not find any significant differences in either slope or intercept between the fog line and LMWL (One-Way ANCOVA,  $p > 0.05$ ). There were also no significant differences between fog  $d$  ( $-0.9\text{‰} \pm 1.2$ ) and LMWL ( $+3.6\text{‰} \pm 8.8$ )

(One-way ANOVA, Welch F test  $p > 0.05$ ), thus we concluded these samples were generated entirely from local meteoric waters, radiation fog ( $\delta^{18}\text{O}$  ( $-0.2\text{‰} \pm 0.4$ ),  $\delta^2\text{H}$  ( $-2.4\text{‰} \pm 2.7$ ) and  $d$  ( $-0.9\text{‰} \pm 1.2$ ) ( $n = 9$ )) (Fig. 2 and Fig. 3) (Kaseke et al., 2017).

The remaining fog samples plotted between the GMWL and LMWL, suggesting admixture of different air masses (Gat and Matsui, 1991; Martinelli et al., 1996; Liu et al., 2007), mixed fog (Kaseke et al., 2017) (Fig. 2). However, the Aussinanis sample plotted to the right of the mixed fog line suggesting evaporative enrichment of the sample (Fig. 2). The enriched isotopic composition and low  $d$  ( $-1.8\text{‰}$ ) of the Aussinanis sample relative to other samples was consistent with this conclusion (Table S1). Therefore we did not characterize mixed fog because the Gobabeb fog sample was the only unevaporated mixed fog sample,  $d$  ( $+5.5\text{‰}$ ). Both mixed fog and radiation fog require similar conditions for formation e.g., radiative cooling and calm winds ( $< 2.5$  m/s) (Roach et al., 1976; Meyer and Lala, 1990; Tardif and Rasmussen, 2007), conditions that were prevalent during the fog events at all sites (Table S2). However, there was a noticeable difference in the degree of radiative cooling and RH during the fog event between the mixed fog sites and the radiation fog sites. Mixed fog sites had a  $6.5^\circ\text{C}$  temperature drop with 94.6% RH while radiation fog sites had a  $3.2^\circ\text{C}$  temperature drop with 98.8% RH (Table S2). The dominant wind direction was variable among sites indicating micro-climatological differences (Table S2).

**[Figure 2 here]**

**[Figure 3 here]**

Kaseke et al. (2017) attributed radiation fog around Gobabeb to local evapotranspiration from the ephemeral Kuiseb River and/or recent rainfall. Vegetation is restricted to ephemeral water courses and the eastern edge of the Namib Desert (Burke, 2006). Therefore, radiation fog originating from groundwater would be restricted to sites along the ephemeral rivers e.g., Stations 1, 2, 5 and Gobabeb, while that from rainfall would be widespread but generally restricted to topographic lows e.g., inter dunes (Eckardt et al., 2013) (Fig. 1). Given the location of the study area, between two ephemeral rivers, transpiration of groundwater by ephemeral vegetation could be a source of moisture that generated this fog. This would account for the similarity between radiation fog  $d$  and LMWL. However, because the area received rainfall on the 6<sup>th</sup> and 7<sup>th</sup> June (Table 1 and Fig. S1), the high soil moisture coupled with conducive micro-climatological conditions at each site could also account for the formation of radiation fog over such a large area (Fig. 3). Therefore, radiation fog on the 10<sup>th</sup> June 2016 could have been derived from either the soil evaporate and/or transpired vapor from the ephemeral rivers. The groundwater isotopic composition of the Swakop River (Marx, 2009) plotted on the LMWL defined for Gobabeb, suggesting similar sources and conditions (Fig. S2).

**[Table 1 here]**

The source isotopic composition of rainfall ( $\delta^{18}\text{O} +3.27\text{‰}$  and  $\delta^2\text{H} +22.34\text{‰}$ ) received on the 6<sup>th</sup> and 7<sup>th</sup> June was enriched relative to radiation fog sampled on the 10<sup>th</sup> June 2016 (Fig. 2). Fog has been reported to be isotopically enriched relative to local rainfall (if they are from the same source) because it is a first stage condensate and formed at generally higher temperatures than rainfall (Gonfiantini and Longinelli, 1962; Ingraham and Matthews, 1988; Scholl et al., 2011). However, local rainfall can be more enriched isotopically than fog in some arid environments because sub-cloud evaporation could result in enrichment beyond that observed in the first stage condensates alone (Kaseke et al., 2017). Backward trajectory analysis of rainfall received on the 6<sup>th</sup> and 7<sup>th</sup> June 2016 showed that both rainfall events originated from the Indian Ocean (Fig. 4). The rain isotopic composition was consistent with enrichment predictions due to sub-cloud evaporation for the Namib Desert since its  $d$  ( $-3.8\text{‰}$ ) was lower than the LMWL ( $+3.6\text{‰}$ ) (Fig. 4) (Kaseke et al., 2016). We thus concluded that fog observed on the 10<sup>th</sup> June 2016 was derived from local meteoric waters through evapotranspiration (Fig. 2).

**[Figure 4 here]**

#### ***Classification of fog on the 17<sup>th</sup> June 2016***

Fog collected on the 17<sup>th</sup> June 2016 was observed at seven sites and the majority of samples showed evidence of evaporative enrichment but plotted close to the LMWL (Fig. 5). This was supported by the significantly lower fog  $d$  ( $-4.1\text{‰} \pm 3.3$ ) compared to the LMWL ( $+3.6\text{‰}$ ) and the low fog yield at Sophies Hoogte, Marble Koppie and Vogelfederberg (Table S3) (One-way

ANOVA, Welch test  $p < 0.05$ ). Therefore we did not characterize the isotopic composition of fog sampled on the 17<sup>th</sup> June. However, we defined a fog evaporation line  $\delta^2\text{H} = 6.24\delta^{18}\text{O} - 5.98$  ( $R^2 = 0.99$ ) for these fog samples and found no significant difference in either slope or intercept between the fog evaporation line and the LMWL (One-way ANCOVA,  $p > 0.05$ ). Coupled with the puddle in Figure S1 which persisted until the 19<sup>th</sup> June 2016, these results suggest that the rainfall events on the 6<sup>th</sup> and 7<sup>th</sup> may have had an ecohydrological impact beyond their onset date. Therefore, we concluded these fog samples were derived from local meteoric waters and classified as radiation fog.

**[Figure 5 here]**

Wind speeds during the fog event on the 17<sup>th</sup> June 2016 were generally calm ( $< 2.5$  m/s) with the exception of Vogelfederberg (Table S2). However, the dominant wind direction for all sites had easterly origins eliminating the ocean as the source because advective fog would have either north-westerly (Seely and Henschel, 1998) or south-westerly origins (Eckardt et al., 2013) (Table S2). Advection-radiation fog is associated with an increase in specific humidity due to inflow from the ocean during the daylight hours (Bari et al., 2016). However, although Vogelfederberg showed an initial increase in specific humidity on the 16<sup>th</sup> June 2016, by end of the daylight hours this had decreased and only increased during the night by  $0.8$  g / kg just before fog onset at 0:00 hrs (Fig. S3). In the hours preceding fog onset, the wind originated from an easterly direction.

The Coastal MET site showed a similar but smaller increase (0.4 g / kg) in specific humidity during the fog event. These results therefore do not support advection-radiation (mixed) fog classification but support our classification of fog on the 17<sup>th</sup> June 2016 being radiation fog.

Fog on the 17<sup>th</sup> June 2016 was restricted to the northern sections of the study area while absent from the southern sections (Fig. 3). Because fog occurs only when particular atmospheric conditions are met (Jacobs et al., 2002), this implies conditions conducive for fog formation were not met in the southern sites on the 17<sup>th</sup> June 2016 (Fig. 3). We analyzed 2016 meteorological data and did not find any significant differences in RH, air and soil temperature (Mann Whitney U tests, Bonferroni  $p > 0.05$ ) among the northern sites or among the southern sites indicating similar meteorological conditions within the northern and southern sites. However, inter-region (north vs south) comparisons showed that RH in the northern sites (66.95%) was significantly higher than in the southern sites (53.60%) (Mann Whitney U test,  $p < 0.05$ ). Air temperature was significantly lower at the northern sites ( $18.87^{\circ}\text{C} \pm 2.6$ ) compared to the southern sites ( $20.72^{\circ}\text{C} \pm 2.4$ ) (ANOVA,  $p < 0.05$ ). There was no significant difference in soil temperature at 10 cm depth between the sites: northern sites ( $24.6^{\circ}\text{C} \pm 3.5$ ) compared to southern sites ( $25.8^{\circ}\text{C} \pm 3.8$ ). These results suggest that conditions in the northern sites were more conducive for radiation fog formation than the southern sites because of the higher RH and lower air temperature. Therefore, we attribute the absence of radiation fog in the southern sites on the 17<sup>th</sup> June, to

microclimatological differences between the northern (cooler and more humid) and southern (warmer and drier) sites (Fig. 3). However, the differences between the northern and southern sites in air temperature and RH could also be due to higher fog frequency at the northern sites.

### ***Classification of fog on the 18<sup>th</sup> June 2016***

Fog on the 18<sup>th</sup> June 2016 was observed at all sites; however, isotopic analysis suggested three types of fog occurred over the area (Fig. 3). Advection fog was observed at four sites, radiation fog at seven sites and mixed fog at one site (Fig. 6). The sample obtained from Station 8 was insufficient for isotopic analysis and was not classified (Fig. 3). Advection fog plotted close but to the right of the GMWL and the advection fog line from Kaseke et al. (2017), suggesting evaporative enrichment of the samples (Fig. 6). The advection fog samples were defined by the regression line  $\delta^2\text{H} = 9.93\delta^{18}\text{O} + 7.74$  ( $R^2 = 0.77$ ) and there was no significant difference in slope between this line and the advection fog line from Kaseke et al. (2017) (ANCOVA,  $p > 0.05$ ). However,  $d$  of these samples (+6‰) was significantly lower than that of the advection fog line (+7.6‰) and GMWL (10‰) (One-way ANOVA, Welch F test,  $p < 0.05$ ), which could be taken as evidence of evaporative enrichment, thus we did not characterize advection fog. Wind data was consistent with this classification, showing westerly and north-westerly origins of fog for Coastal MET and Kleinberg stations (Fig. 3 and Table S2).

Computing forward trajectories of advection fog observed at Coastal MET and Kleinberg based on the dominant winds, we expected the fog to extend to Sophies Hoogte (~50 km inland) but the



sample obtained from Sophies Hoogte was classified as mixed fog based on isotopes (Fig. 6). This suggests either, dissipation of advective fog downwind and the mixing of residual humidity with locally derived moisture followed by radiative cooling of the mixed air mass to generate mixed fog, or, advective fog incorporating substantial amounts of local moisture along its inland trajectory altering its isotopic composition to that of mixed fog while maintaining the same RH (Fig. 3 and Table S2). The dominant wind direction at Sophies Hoogte ( $342^\circ$ ) suggests advective fog or residual moisture may have entered the Namib Desert north of the Swakop River, incorporating transpired vapor along the river transforming into mixed fog as it extended southwards (Fig. 1 and Table S2). As the fog extended south, it may have also incorporated soil evaporate (Fig. S1), resulting in the mixed fog isotopic composition of the sample obtained from Sophies Hoogte (Fig. 3).

**[Figure 6 here]**

Seven fog samples from the 18<sup>th</sup> June were classified as locally generated, radiation fog samples (Fig. 3). Three samples plotted directly on the LMWL consistent with local origins of fog ( $\delta^{18}\text{O}$  -2.8‰,  $\delta^2\text{H}$  -20.1‰), while the remaining plotted to the right of the LMWL suggesting evaporative enrichment and were excluded from isotopic characterization (Fig. 6). Radiation fog  $d$  ( $+2.1\text{‰} \pm 0.6$ ) was similar to LMWL ( $+3.6\text{‰} \pm 8.8$ ) (One-way ANOVA, Welch F test  $p > 0.05$ ) suggesting local origins of the fog. Interestingly, all sites classified as having received

radiation fog had on average lower RH during the fog event than sites with samples classified as advective and mixed fog (Fig. 3 and Table S2).

Marble Koppie was dominated by westerly winds during the fog event, suggesting extension of mixed fog further inland (~60 km), but the isotopic composition was consistent with local origins (Fig. 3 and Table S2). Coupled with the decrease in RH, these results suggest that the advecting mixed fog/moisture incorporated more local moisture increasing its contribution while RH decreased. This resulted in a change in the isotopic composition to reflect the dominance of the local moisture contribution to fog ~60 km inland, radiation fog (Fig. 3 and Fig. 6). Taking into account the west-east and north-south wind trajectories during the fog occurrence at Kleinberg and Sophies Hoogte, respectively (Table S2), it suggests convergence of these systems about 50 km inland, extending fog in a south-easterly direction to about 60 km inland (Fig. 3). However, fog samples obtained from sites 60 km inland were classified as radiation fog, suggesting that either the fog observed at Sophies Hoogte dissipated before 60 km and the fog observed at these sites was generated from local moisture (6<sup>th</sup> and 7<sup>th</sup> June rains) or the mixed fog observed at Sophies Hoogte incorporated more local moisture along its trajectory inland altering the isotopic composition to that of radiation fog (Fig. 3 and Fig. 6). The dominant winds during the fog event at the southern sites (~60 km inland) was variable e.g., Gobabeb and Station 8 had southerly origins, Aussinanis (north-westerly) while Vogelfederberg had easterly origins (Table

S2). The southerly wind origins at Gobabeb suggest that transpiration from the Kuiseb River may have contributed moisture to radiation fog (Fig. 1 and Fig. 3).

Interestingly, Station 2 (~30 km inland, 215 m a.s.l) was classified as radiation fog and received less input than Stations 3 and 4 (~ 33 km inland, 185 m a.s.l) which were classified as advective fog (Fig. 3 and Table S4). This suggests substantial amounts of locally derived moisture was added to advective fog/moisture within ~30 km from the coast, altering the isotopic composition to reflect the dominance of the local moisture input component to the fog observed at Station 2 (Fig. 3). This local moisture could have been generated from the residual soil moisture (6<sup>th</sup> and 7<sup>th</sup> June rains) and the ephemeral vegetation given the proximity of Station 2 to the Kuiseb River (Fig. 1). Similarly, the fog samples from Station 1, 5 and Gobabeb located along the Kuiseb River were also classified as locally generated fog (Fig. 1 and Fig. 3).

These results suggest that the observed widening or extension of the Namib fog-zone to about 60 km inland between the Swakop and Kuiseb rivers could be due to the perpetuation of ‘advective’ fog by evapotranspiration from river vegetation in addition to the effect of topography (Lancaster, 1984; Cermak, 2012) (Fig. 1).

### ***Classification of fog on the 19<sup>th</sup> June 2016***

Fog on the 19<sup>th</sup> June 2016 was experienced at all 13 stations. However, there was insufficient sample for analysis from the Coastal MET station (Fig. 3). The five fog samples classified as mixed fog:  $\delta^{18}\text{O}$  ( $-1.1\text{‰} \pm 0.4$ ),  $\delta^2\text{H}$  ( $-5.1\text{‰} \pm 3.4$ ) and  $d$  ( $+3.9\text{‰} \pm 0.8$ ) (Fig. 3 and Fig. 7) were

restricted to the northern sites (Fig. 3). Although mixed fog  $d$  (+3.9‰) was not significantly larger than the LMWL (+3.6‰) (One-way ANOVA, Welch F test,  $p > 0.05$ ), the samples plotted between the GMWL and LMWL on the mixed fog line from Kaseke et al. (2017) suggesting admixture of different air masses, mixed fog (Fig. 7). Although somewhat similar to the 18<sup>th</sup> June fog, the fog on the 19<sup>th</sup> June was unique in that local moisture inputs to advective moisture/fog was substantial to alter the isotopic composition of the fog at all northern sites, to form mixed fog (Fig. 3). Because the fog yield on the 19<sup>th</sup> was generally lower than on the 18<sup>th</sup> June 2016, suggests a light advective fog (low precipitable water) and the local moisture additions along the trajectory increased the fog precipitable water resulting in a west-east increasing fog yield gradient (Table S3).

All fog samples collected from the southern sites plotted on the LMWL and there was no significant difference between fog  $d$  (+0.1‰  $\pm$  1.2) and LMWL (+3.6‰), hence classified as radiation fog ( $\delta^{18}\text{O}$  (-1.3‰  $\pm$  1.7),  $\delta^2\text{H}$  (-10.5‰  $\pm$  3.9)) (Fig. 3 and Fig. 7). This fog may have been formed by radiative cooling of moisture derived from local waters as wind directions were variable among sites while wind speeds at each site were consistent with those associated with radiation fog (< 2.5 m/s) (Roach et al., 1976; Meyer and Lala, 1990; Tardif and Rasmussen, 2007) (Table S2). Or this fog is formed by the perpetuation of mixed fog inland with addition of local moisture along its trajectory similar to that proposed for the 18<sup>th</sup> June 2016. Therefore,

although fog observed over the area on the 19<sup>th</sup> June may appear like a single fog event, the isotopic data suggests this was composed of mixed fog in the northern sections and radiation fog in the southern sites (Fig. 3).

**[Figure 7 here]**

### ***The relationships between radiation fog isotopic compositions and physical factors***

We analyzed meteorological data of all FN radiation fog samples that did not show evidence of evaporative enrichment (plotted on the LMWL) and defined these as  $\delta^2\text{H} = 7.15 \times \delta^{18}\text{O} - 1.42$  ( $R^2 = 0.99$ ,  $n = 13$ ). There was no significant difference between the LMWL and the radiation fog line in either slope or intercept (One-way ANCOVA,  $p > 0.05$ ). There was also no significant difference between the  $d$  of the LMWL ( $+3.6\text{‰}$ ) and the radiation fog line ( $-0.1\text{‰} \pm 1.6$ ) (One-way ANOVA Welch F test,  $p > 0.05$ ). Therefore we concluded that these fog samples were derived from local meteoric waters.

Our results show that radiation fog  $\delta^{18}\text{O}$  and  $\delta^2\text{H}$  were positively correlated with soil temperature (at 10 cm depth) ( $p < 0.05$ ) (Fig. 8a and Fig. 8b). The recent rains received over the area (Table 1 and Fig. 4) resulted in saturation of the soil surface with surface storage at some sites (Fig. S1). However, these soils were exposed to evaporative conditions, which resulted in drying of the soil, creating unsaturated conditions from the surface. Overtime, soil tortuosity increases and vapor movement becomes the dominant avenue for water transfer to the surface (Philip, 1957). Vapor movement in arid soils is an important means of water transfer (Evans and

Thames, 1981) and nocturnal cooling may generate a thermal gradient sufficient for upward vapor movement from soil to atmosphere (Philip, 1957; Francis et al., 2007). On average, our sites show a 4.9°C nighttime soil-atmosphere temperature gradient during radiation fog events, which would facilitate nighttime evaporation from the soil (Table S2). Soil water becomes enriched in both  $^{18}\text{O}$  and  $^2\text{H}$  at the soil surface due to evaporation that is dominated by kinetic fractionation effects (Allison and Barnes, 1983). The resulting vapor transferred into the atmosphere is thus isotopically depleted in  $^{18}\text{O}$  and  $^2\text{H}$  compared to the soil water. Condensation of this vapor during fog formation (equilibrium fractionation) results in a condensate that is depleted in  $^{18}\text{O}$  and  $^2\text{H}$  compared to the soil water or rain (Fig. 2). As soil temperatures increase, kinetic fractionation effects are reduced causing an increase in  $\delta^{18}\text{O}$  and  $\delta^2\text{H}$  in the vapor and consequently  $^{18}\text{O}$  and  $^2\text{H}$  enrichment in fog condensed from this vapor (Fig. 8a and Fig. 8b). Interestingly, we did not find any significant correlation between radiation fog  $\delta^{18}\text{O}$  and  $\delta^2\text{H}$  and air temperature.

**[Figure 8 here]**

Radiation fog  $\delta^{18}\text{O}$  and  $\delta^2\text{H}$  was also positively correlated with RH (Fig. 8c and Fig. 8d) ( $p < 0.05$ ). Since the observed radiation fog was likely derived from soil moisture, this means RH was related to the amount of soil moisture transferred into the atmosphere. Because evaporation from the drying soil is dominated by kinetic fractionation effects resulting in a vapor depleted in  $^{18}\text{O}$

and  $^2\text{H}$ , condensation at low humidity results in fog with low  $\delta^{18}\text{O}$  and  $\delta^2\text{H}$  values. However, as more moisture is transferred into the atmosphere increasing RH, this also increases vapor  $\delta^{18}\text{O}$  and  $\delta^2\text{H}$  values and condensation of this vapor under equilibrium conditions should result in an increase in  $\delta^{18}\text{O}$  and  $\delta^2\text{H}$  in the resulting condensate (Fig. 8c and Fig. 8d).

We acknowledge the limitations of our study such as the limited dataset and the unusually large winter rainfall, which may not reflect typical conditions over the study area. However, despite these limitations, this study demonstrated that besides advective fog, radiation and mixed fog occurred regularly in this section of the Namib Desert, at least during the observation period. Furthermore, stable isotope analysis of fog suggests co-occurrence of different types of fog during what appears as a single fog event over a large geographic area, similar to the observations of Bari et al. (2016) in Morocco. This suggests that our current understanding of fog dominated ecosystems could be overly simplistic thus there is a need for further studies to understand spatial variability of fog types, their significance to ecohydrology and how shifts or changes might affect the composition of endemic flora and fauna in the future. The study also suggests a north-south decreasing fog gradient similar to that reported by Olivier (1995).

## CONCLUSIONS

Local precipitation over the Namib Desert had impacts on fog formation beyond their onset resulting in localized fog, radiation fog. Formation of this localized fog was dependent on micro-

climatological conditions at each site and occurred more frequently in the more humid and cooler northern sites compared to the southern sites. Evapotranspiration from the Swakop and Kuiseb rivers could be influential in perpetuating fog inland, creating the observed extension / bulge of the fog-zone inland, in the area between these ephemeral rivers. It is important to acknowledge the short span of the observations in this study, thus future studies using this novel isotope framework are needed to confirm the observed spatial trend. Nonetheless, isotope analyses have demonstrated spatial variations of fog over this area and that what appears as a single fog event may be a mix of different fog types with different formation processes. Such information is particularly important for the Namib Desert because the response of fog dependent desert organisms to climate change is dependent or linked to the source of the fog: ocean or locally generated.

## **ACKNOWLEDGMENTS**

We would like to acknowledge Gobabeb Research and Training Centre for access to the FogNet weather stations and for the logistical support and fieldwork assistance. We would also like to thank Dr. Jia Hu, Dr. Martha Stroll and one anonymous reviewer for their constructive comments to improve the quality of this manuscript. Funding for this work was made available from the U.S. National Science Foundation (IIA-1427642 and EAR-1554894).



## **DISCLAIMER**

Reference to any companies or specific commercial products does not constitute an endorsement of these products.

## REFERENCES

- Agam, N. and Berliner, P. (2006). Dew formation and water vapor adsorption in semi-arid environments—a review. *Journal of Arid Environments* 65: 572-590.
- Allison, G. and Barnes, C. (1983). Estimation of evaporation from non-vegetated surfaces using natural deuterium.
- Bari, D., Bergot, T. and El Khelifi, M. (2016). Local meteorological and large-scale weather characteristics of fog over the grand casablanca region, morocco. *Journal of Applied Meteorology and Climatology* 55: 1731-1745.
- Berry, F.A., Bollay, E. and Beers, N.R. (1945). Handbook of meteorology.
- Burke, A. (2006). Savanna trees in namibia - factors controlling their distribution at the arid end of the spectrum. *Flora* 201: 189-201.
- Byers, H.R. (1959). General meteorology, In *General meteorology*, McGraw-Hill.
- Cereceda, P., Osses, P., Larrain, H., Farias, M., Lagos, M., Pinto, R. and Schemenauer, R. (2002). Advective, orographic and radiation fog in the tarapacá region, chile. *Atmospheric Research* 64: 261-271.
- Cermak, J. (2012). Low clouds and fog along the south-western african coast—satellite-based retrieval and spatial patterns. *Atmospheric Research* 116: 15-21.
- Dansgaard, W. (1964). Stable isotopes in precipitation. *Tellus*, 16: 436-468.
- Dawson, T.E. (1998). Fog in the california redwood forest: Ecosystem inputs and use by plants. *Oecologia* 117: 476-485.
- Degefie, D., El-Madany, T.-S., Hejkal, J., Held, M., Dupont, J.-C., Haeffelin, M. and Klemm, O. (2015). Microphysics and energy and water fluxes of various fog types at sirta, france. *Atmospheric Research* 151: 162-175.
- Ebner, M., Miranda, T. and Roth-Nebelsick, A. (2011). Efficient fog harvesting by stipagrostis sabulicola (namib dune bushman grass). *Journal of Arid Environments* 75: 524-531.
- Eckardt, F., Soderberg, K., Coop, L., Muller, A., Vickery, K., Grandin, R., Jack, C., Kapalanga, T. and Henschel, J. (2013). The nature of moisture at gobabeb, in the central namib desert. *Journal of Arid Environments* 93: 7-19.
- Evans, D.D. and Thames, J.L. (1981). Water in desert ecosystems. *Water in Desert Ecosystems*.
- Francis, M., Fey, M., Prinsloo, H., Ellis, F., Mills, A. and Medinski, T. (2007). Soils of namaqualand: Compensations for aridity. *Journal of Arid Environments* 70: 588-603.
- Gat, J. (2005). Some classical concepts of isotope hydrology, In *Isotopes in the water cycle*, Springer, pp. 127-137.
- Gat, J. and Matsui, E. (1991). Atmospheric water balance in the amazon basin: An isotopic evapotranspiration model. *Journal of Geophysical Research: Atmospheres* 96: 13179-13188.
- George, J.J. (1951). Fog, In *Compendium of meteorology*, Springer, pp. 1179-1189.
- Gonfiantini, R. and Longinelli, A. (1962). Oxygen isotopic composition of fogs and rains from the north atlantic. *Experientia* 18: 222-223.

- Gultepe, I., Pagowski, M. and Reid, J. (2007a). A satellite-based fog detection scheme using screen air temperature. *Weather and forecasting* 22: 444-456.
- Gultepe, I., Tardif, R., Michaelides, S., Cermak, J., Bott, A., Bendix, J., Müller, M., Pagowski, M., Hansen, B. and Ellrod, G. (2007b). Fog research: A review of past achievements and future perspectives. *Pure and Applied Geophysics* 164: 1121-1159.
- Hachfeld, B., Jürgens, N., Deil, U. and Loidi, J. In (Ed.)<sup>(Eds.)</sup> Vegetation and climate. A selection of contributions presented at the 42nd Symposium of the International Association of Vegetation Science, Bilbao, Spain, 26-30 July 1999., 2000, Gebrüder Borntraeger Verlagsbuchhandlung, pp. 567-589.
- Henschel, J.R. and Seely, M.K. (2008). Ecophysiology of atmospheric moisture in the namib desert. *Atmospheric Research* 87: 362-368.
- Ingraham, N.L. and Matthews, R.A. (1988). Fog drip as a source of groundwater recharge in northern kenya. *Water Resources Research* 24: 1406-1410.
- Ingraham, N.L. and Matthews, R.A. (1990). A stable isotopic study of fog: The point reyes peninsula, california, u.S.A. *Chemical Geology: Isotope Geoscience section* 80: 281-290.
- Jacobs, A.F., Heusinkveld, B.G. and Berkowicz, S.M. (2002). A simple model for potential dewfall in an arid region. *Atmospheric Research* 64: 285-295.
- Jacobson, K., van Diepeningen, A., Evans, S., Fritts, R., Gemmel, P., Marsho, C., Seely, M., Wenndt, A., Yang, X. and Jacobson, P. (2015). Non-rainfall moisture activates fungal decomposition of surface litter in the namib sand sea.
- Jouzel, J. (1986). Isotopes in cloud physics: Multiphase and multistage condensation processes. *Handbook of Environmental Isotope Geochemistry* 2: 61-112.
- Kaseke, K.F., Wang, L. and Seely, M.K. (2017). Nonrainfall water origins and formation mechanisms. *Science Advances* 3: e1603131.
- Kaseke, K.F., Wang, L., Wanke, H., Turewicz, V. and Koeniger, P. (2016). An analysis of precipitation isotope distributions across namibia using historical data. *PloS one* 11.
- Lancaster, M. (1984). Climate of the central namib desert. *Madoqua* 14: 5-61.
- Lange, J. (2005). Dynamics of transmission losses in a large and stream channel. *Journal of Hydrology* 306: 112-126.
- Limm, E.B., Simonin, K.A., Bothman, A.G. and Dawson, T.E. (2009). Foliar water uptake: A common water acquisition strategy for plants of the redwood forest. *Oecologia* 161: 449-459.
- Liu, W.J., Liu, W.Y., Li, P.J., Gao, L., Shen, Y.X., Wang, P.Y., Zhang, Y.P. and Li, H.M. (2007). Using stable isotopes to determine sources of fog drip in a tropical seasonal rain forest of xishuangbanna, sw china. *Agricultural and Forest Meteorology* 143: 80-91.
- Majoube, M. (1971).  $\Delta^{18}\text{O}$  and deuterium fractionation between water and steam *Journal De Chimie Physique Et De Physico-Chimie Biologique* 68: 1423.

- Martinelli, L.A., Victoria, R.L., Sternberg, L.S.L., Ribeiro, A. and Moreira, M.Z. (1996). Using stable isotopes to determine sources of evaporated water to the atmosphere in the amazon basin. *Journal of hydrology* 183: 191-204.
- Marx, V. (2009). Impacts of upstream uses on the alluvial aquifer of the swakop river, namibia. *Germany: Diplomarbeit, Albert Ludwig University of Freiburg.*
- Merlivat, L. and Jouzel, J. (1979). Global climatic interpretation of the deuterium-18o relationship for precipitation. *J. Geophys. Res.* 84: 5029-5033.
- Meyer, M.B. and Lala, G.G. (1990). Climatological aspects of radiation fog occurrence at albany, new york. *Journal of Climate* 3: 577-586.
- Nørgaard, T., Ebner, M. and Dacke, M. (2012). Animal or plant: Which is the better fog water collector? *PloS one* 7: e34603.
- Olivier, J. (1995). Spatial distribution of fog in the namib. *Journal of Arid Environments* 29: 129-138.
- Olivier, J. (2004). Fog-water harvesting along the west coast of south africa: A feasibility study. *Water SA* 28: 349-360.
- Philip, J.R. (1957). Evaporation, and moisture and heat fields in the soil. *Journal of meteorology* 14: 354-366.
- Roach, W., Brown, R., Caughey, S., Garland, J. and Readings, C. (1976). The physics of radiation fog: I—a field study. *Quarterly Journal of the Royal Meteorological Society* 102: 313-333.
- Ryznar, E. (1977). Advection-radiation fog near lake michigan. *Atmospheric Environment* (1967) 11: 427-430.
- Salati, E., Dall'Olio, A., Matsui, E. and Gat, J.R. (1979). Recycling of water in the amazon basin: An isotopic study. *Water Resources Research* 15: 1250-1258.
- Schachtschneider, K. and February, E.C. (2010). The relationship between fog, floods, groundwater and tree growth along the lower kuiseb river in the hyperarid namib. *Journal of Arid Environments* 74: 1632-1637.
- Schemenauer, R.S. and Cereceda, P. (1991). Fog-water collection in arid coastal locations. *Ambio*: 303-308.
- Schemenauer, R.S. and Cereceda, P. (1994). A proposed standard fog collector for use in high-elevation regions. *Journal of Applied Meteorology* 33: 1313-1322.
- Scholl, M., Eugster, W. and Burkard, R. (2011). Understanding the role of fog in forest hydrology: Stable isotopes as tools for determining input and partitioning of cloud water in montane forests. *Hydrological Processes* 25: 353-366.
- Scholl, M.A., Gingerich, S.B. and Tribble, G.W. (2002). The influence of microclimates and fog on stable isotope signatures used in interpretation of regional hydrology: East maui, hawaii. *Journal of Hydrology* 264: 170-184.
- Schulze, B. (1969). The climate of gobabeb. *Scientific Papers of the Namib Desert Research Station* 1969: 5-12.
- Seely, M. (1979). Irregular fog as a water source for desert dune beetles. *Oecologia* 42: 213-227.
- Seely, M. and Henschel, J. In (Ed.)^(Eds.) Proceedings of the First International Conference on Fog and Fog Collection, 1998, pp. 19-24.
- Simonin, K.A., Santiago, L.S. and Dawson, T.E. (2009). Fog interception by sequoia sempervirens (d. Don) crowns decouples physiology from soil water deficit. *Plant, cell & environment* 32: 882-892.

- Soderberg, K., Good, S.P., O'Connor, M., Wang, L., Ryan, K. and Caylor, K.K. (2013). Using atmospheric trajectories to model the isotopic composition of rainfall in central kenya. *Ecosphere* 4: art33.
- Stein, A., Draxler, R., Rolph, G., Stunder, B., Cohen, M. and Ngan, F. (2015). Noaa's hysplit atmospheric transport and dispersion modeling system. *Bulletin of the American Meteorological Society* 96: 2059-2077.
- Stewart, M.K. (1975). Stable isotope fractionation due to evaporation and isotopic exchange of falling waterdrops: Applications to atmospheric processes and evaporation of lakes. *Journal of Geophysical Research* 80: 1133-1146.
- Tardif, R. and Rasmussen, R.M. (2007). Event-based climatology and typology of fog in the new york city region. *Journal of applied meteorology and climatology* 46: 1141-1168.
- Wang, L., Caylor, K. and Dragoni, D. (2009). On the calibration of continuous, high-precision  $\delta^{18}\text{O}$  and  $\delta^2\text{H}$  measurements using an off-axis integrated cavity output spectrometer *Rapid Communications in Mass Spectrometry* 23: 530-536.
- Wang, L., Caylor, K.K., Villegas, J.C., Barron-Gafford, G.A., Breshears, D.D. and Huxman, T.E. (2010). Partitioning evapotranspiration across gradients of woody plant cover: Assessment of a stable isotope technique. *Geophysical Research Letters* 37.
- Wang, L., Good, S.P., Caylor, K.K. and Cernusak, L.A. (2012). Direct quantification of leaf transpiration isotopic composition. *Agricultural and Forest Meteorology* 154-155: 127-135.
- Wang, L., Kaseke, K.F. and Seely, M.K. (2017). Effects of non-rainfall water inputs on ecosystem functions. *WIREs* 30: 2077–2086 doi:10.1002/wat1002.1179.
- Weathers, K.C. and Likens, G.E. (1996). Clouds in southern chile: An important source of nitrogen to nitrogen-limited ecosystems? *Environmental Science & Technology* 31: 210-213.
- WMO (1992). *International meteorological vocabulary*, 2 ed. World Meteorological Organization.

**Table 1** Rainfall amounts recorded at each FogNet site in the Central Namib Desert, June 2016.

Site	6 June 2016	7 June 2016
	Rainfall (mm)	Rainfall (mm)
Coastal MET	2.4	1.7
Kleinberg	3.8	0.3
Sophies Hoogte	4.7	3.7
Marble Koppie	4.4	3.0
Vogelfedeberg	3.1	4.6
Station 8	4.4	9.0
Aussinanis	3.7	13.3
Gobabeb	3.8	8.7

## Figure Captions

**Fig. 1.** Map indicating the location and extent of the Namib Desert and Namib fog-zone in southern Africa, with the spatial distribution of the individual sampling stations. FN (FogNet) denotes a station that is part of the SASSCAL network and the photo shows a typical setup of the automated weather station. The Swakop River groundwater sampling points were obtained from Marx (2009).

**Fig. 2.** Isotopic classification of fog samples collected from 10 sites in the Central Namib Desert on the 10<sup>th</sup> June 2016 into mixed fog and radiation fog. The GMWL, LMWL, and radiation fog line were used as references and adapted from Kaseke et al. (2017).

**Fig. 3.** Temporal and spatial variation of fog classification in the Central Namib Desert, June 2016.

**Fig. 4.** Map of Southern Africa showing origins of rain that fell over the Central Namib Desert on the 6<sup>th</sup>, 7<sup>th</sup> and 14<sup>th</sup> June 2016. These trajectories were calculated using HYSPLIT for each of the eight FogNet stations that were included in the study.

**Fig. 5.** Isotopic classification of fog samples collected from the Central Namib Desert on the 17<sup>th</sup> June 2016. The GMWL, LMWL, and radiation fog line were used as references and adapted from Kaseke et al. (2017).

**Fig. 6.** Isotopic classification of fog samples collected from 12 sites in the Central Namib Desert on the 18<sup>th</sup> June 2016 into advective fog, mixed fog and radiation fog. The GMWL, LMWL, advective fog line, mixed fog line and radiation fog line were used as references and adapted from Kaseke et al. (2017).

**Fig. 7.** Isotopic classification of fog samples collected from 13 sites in the Central Namib Desert on the 19<sup>th</sup> June 2016 into mixed and radiation fog types. The GMWL, LMWL, mixed fog line and radiation fog line were used as references and adapted from Kaseke et al. (2017).

**Fig. 8.** The relationship between soil temperature at 10 cm depth and radiation fog isotopes a)  $\delta^{18}\text{O}$  and b)  $\delta^2\text{H}$ . The relationship between relative humidity and radiation fog c)  $\delta^{18}\text{O}$  and d)  $\delta^2\text{H}$ .



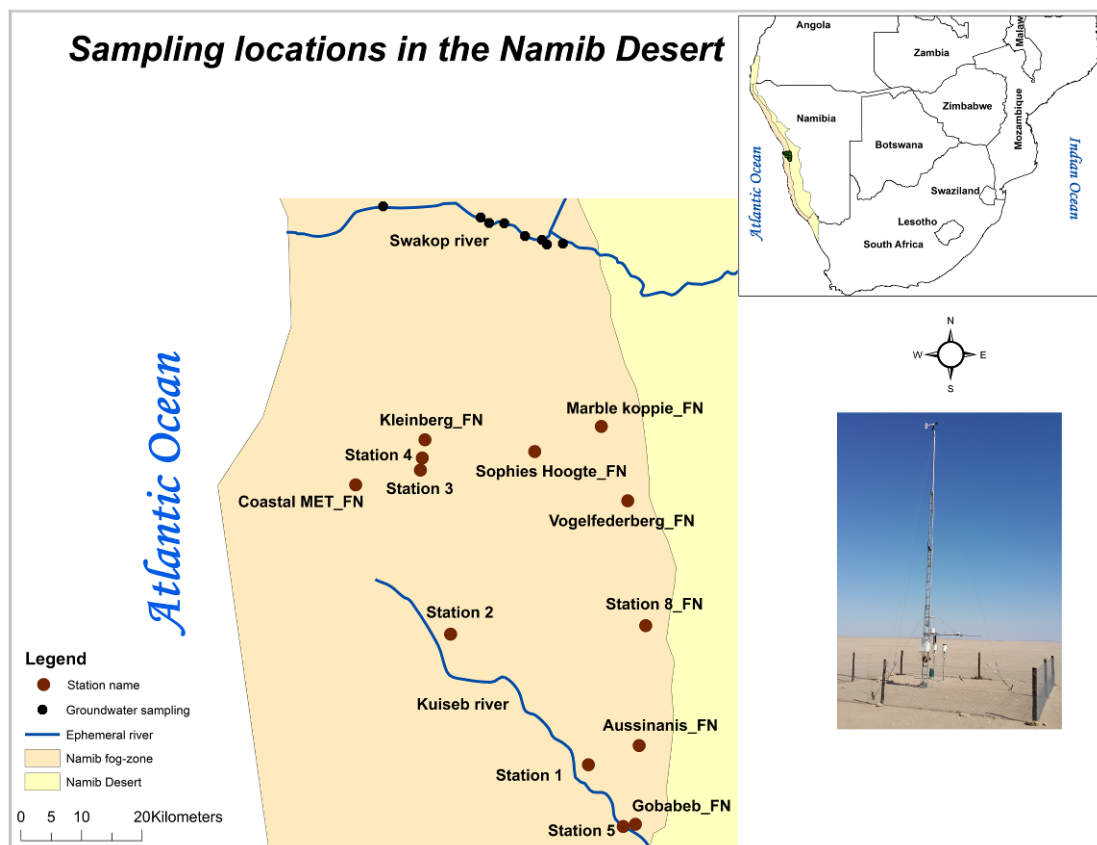


**Fig. 1**

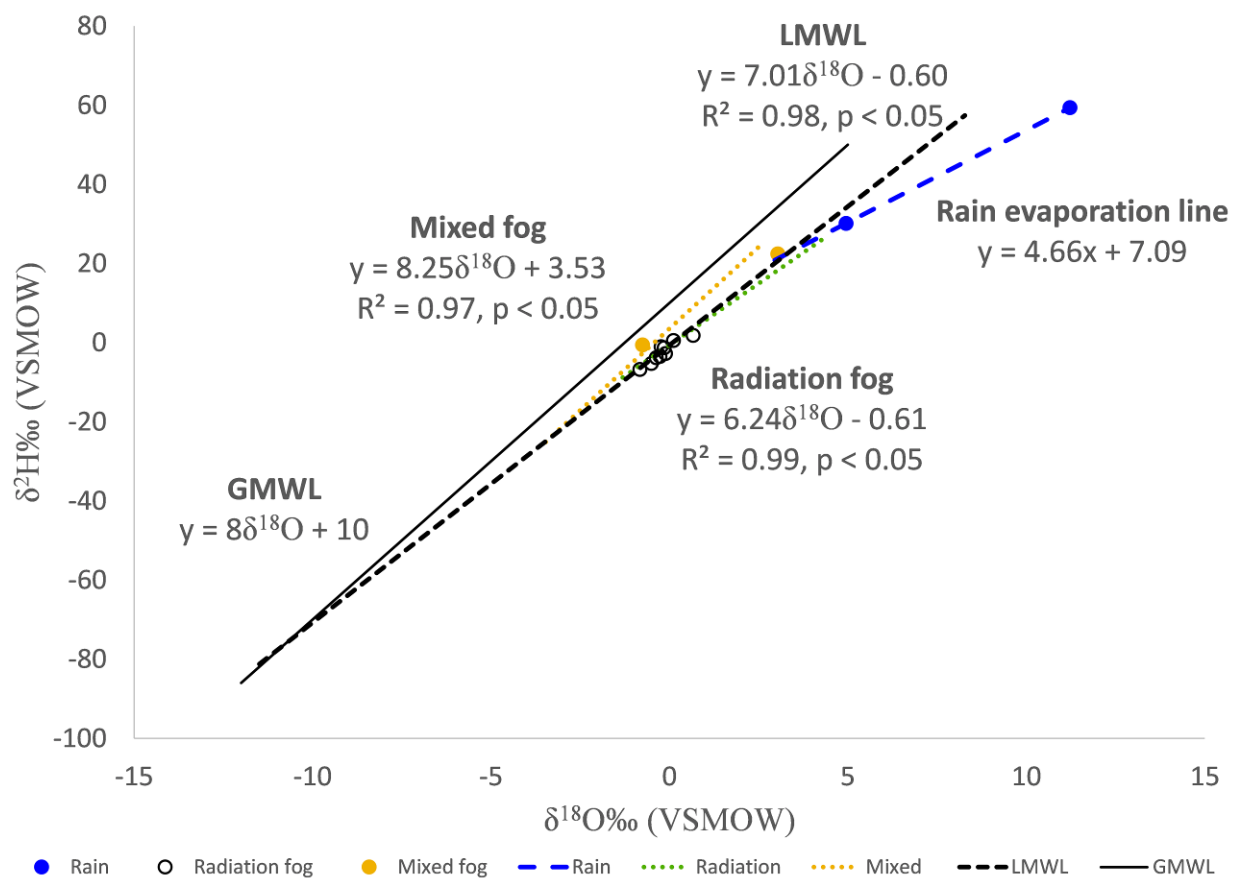


**Fig. 2**



**Fig. 3**

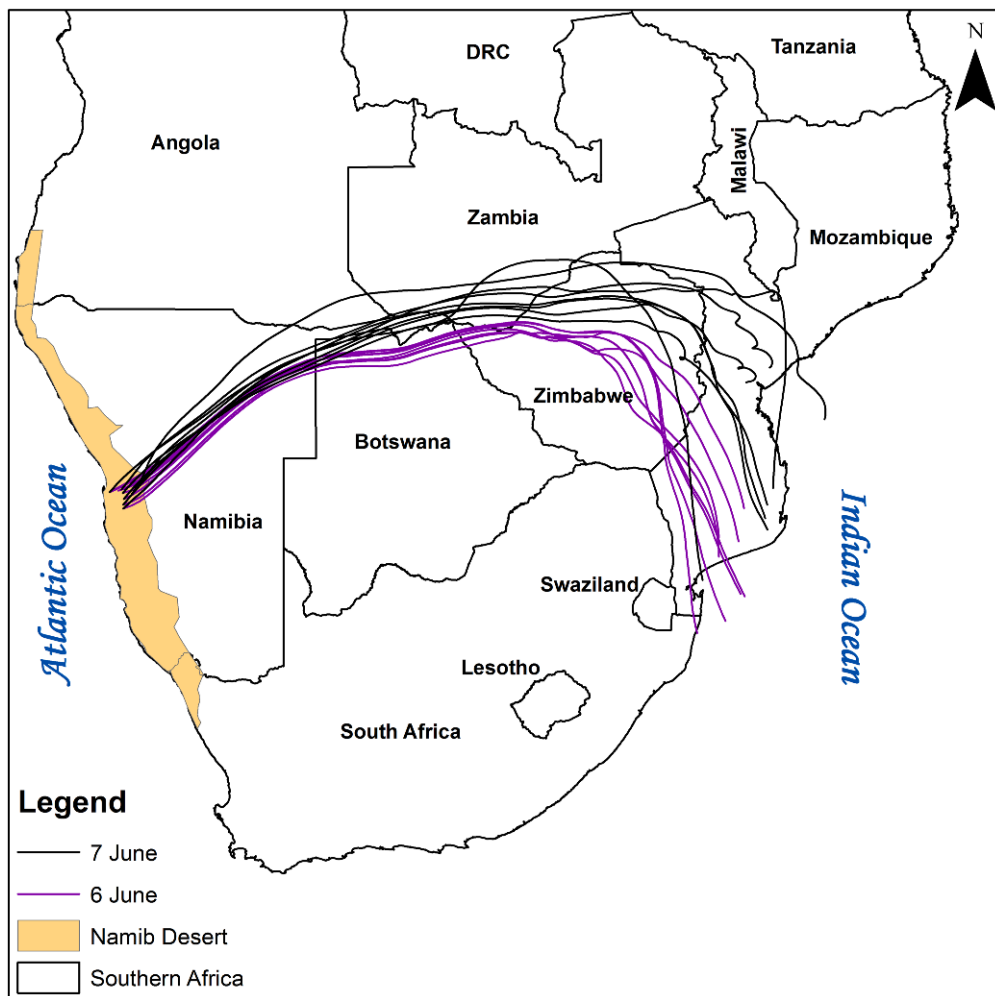


**Fig. 4**

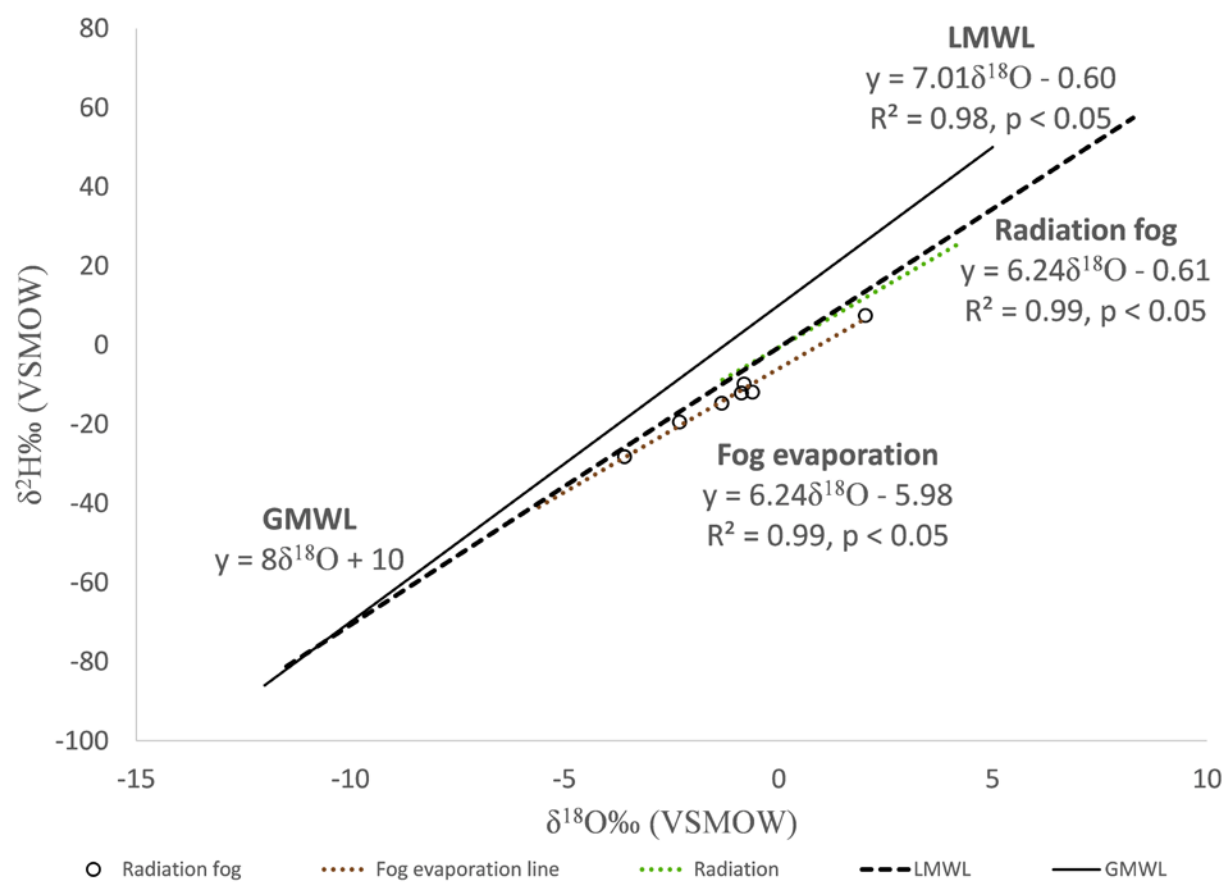


**Fig. 5**

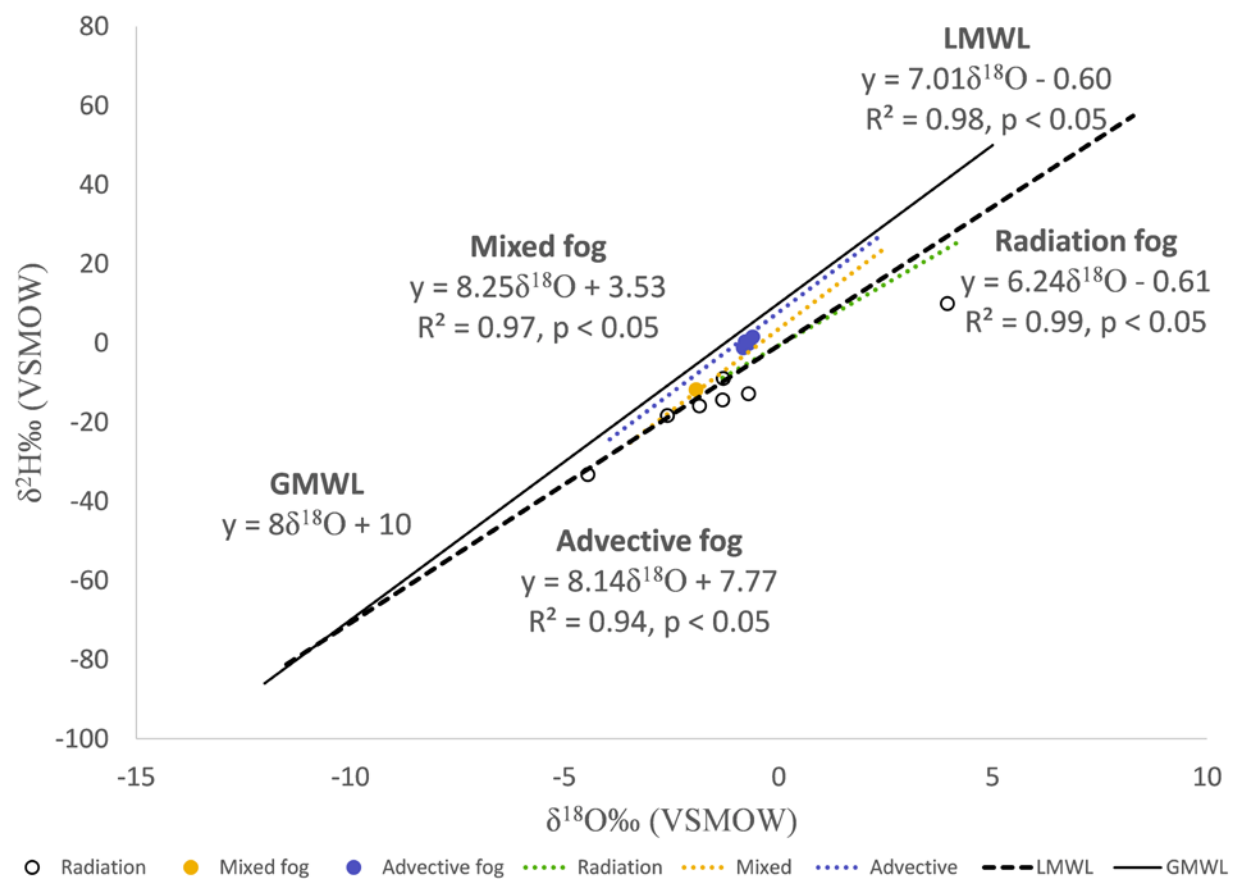


**Fig. 6**

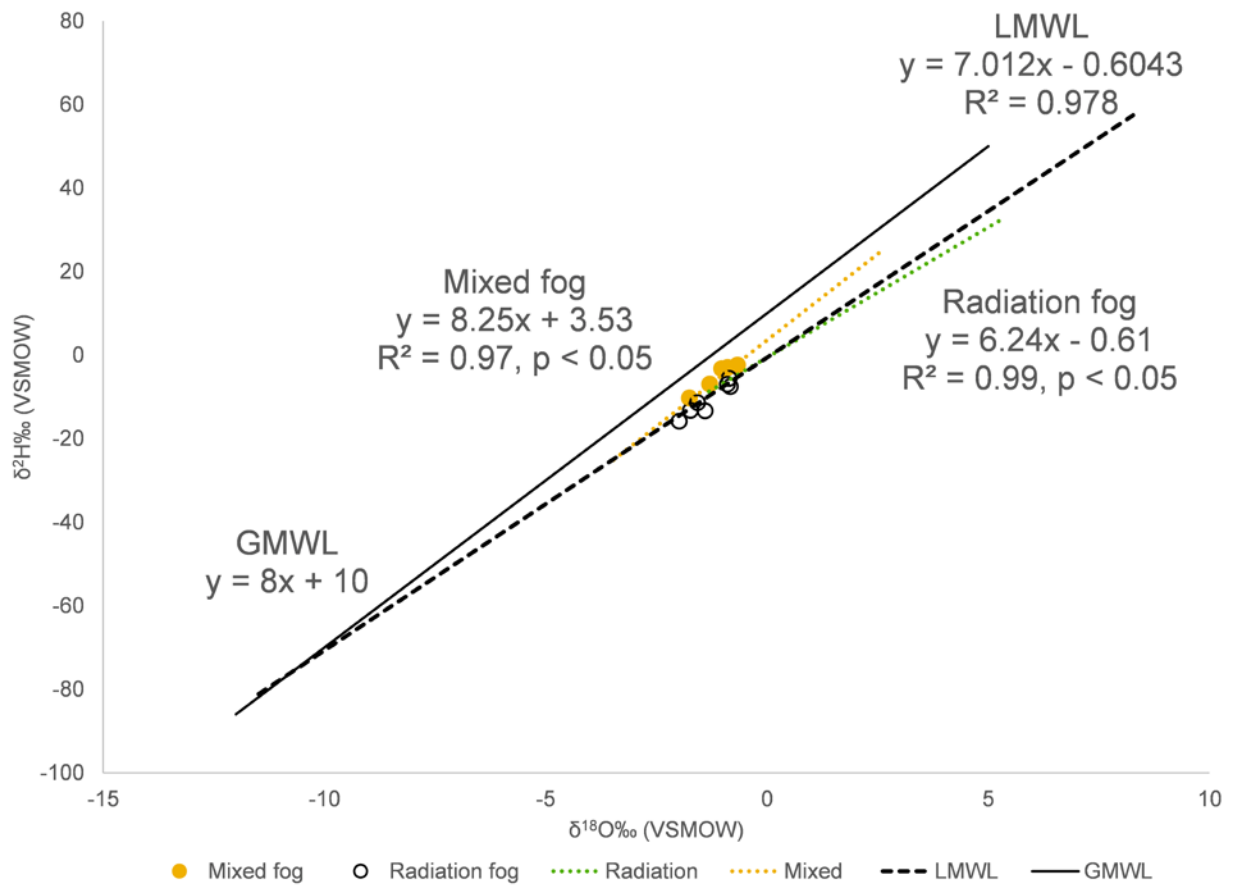


**Fig. 7**

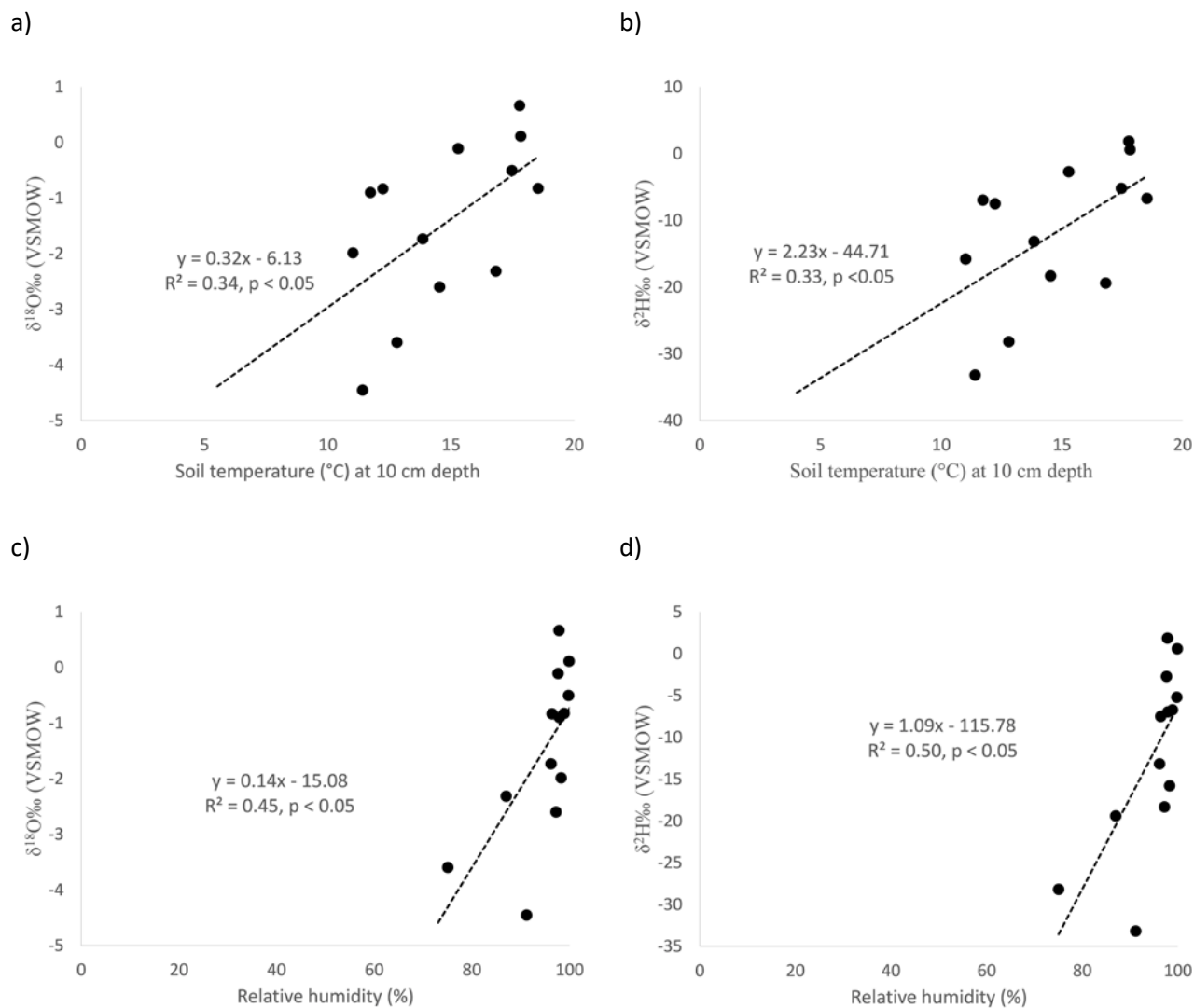


**Fig. 8**